

RESEARCH

Open Access



Inhibition of SARS-CoV-2 infection in human airway epithelium with a xeno-nucleic acid aptamer

Niayesh Razi¹, Weizhong Li², Maxinne A. Ignacio¹, Jeffrey M. Loubé¹, Eva L. Agostino¹, Xiaoping Zhu², Margaret A. Scull^{1*} and Jeffrey J. DeStefano^{1*}

Abstract

Background SARS-CoV-2, the agent responsible for the COVID-19 pandemic, enters cells through viral spike glycoprotein binding to the cellular receptor, angiotensin-converting enzyme 2 (ACE2). Given the lack of effective antivirals targeting SARS-CoV-2, we previously utilized systematic evolution of ligands by exponential enrichment (SELEX) and selected fluoro-arabino nucleic acid (FANA) aptamer R8-9 that was able to block the interaction between the viral receptor-binding domain and ACE2.

Methods Here, we further assessed FANA-R8-9 as an entry inhibitor in contexts that recapitulate infection in vivo.

Results We demonstrate that FANA-R8-9 inhibits spike-bearing pseudovirus particle uptake in cell lines. Then, using an in-vitro model of human airway epithelium (HAE) and SARS-CoV-2 virus, we show that FANA-R8-9 significantly reduces viral infection when added either at the time of inoculation, or several hours later. These results were specific to the R8-9 sequence, not the xeno-nucleic acid utilized to make the aptamer. Importantly, we also show that FANA-R8-9 is stable in HAE culture secretions and has no overt cytotoxic effects.

Conclusions Together, these results suggest that FANA-R8-9 effectively prevents infection by specific SARS-CoV-2 variants and indicate that aptamer technology could be utilized to target other clinically-relevant viruses in the respiratory mucosa.

Keywords FANA, Aptamer, SARS-CoV-2, Human airway epithelium

Background

Severe acute respiratory syndrome coronavirus 2 (SARS-CoV-2), the causative agent of COVID-19, has had a devastating impact on society, resulting in nearly 7 million deaths and over 750 million reported infections worldwide. Through vaccination, natural virus evolution, surveillance, and better treatment protocols, the pandemic has dramatically declined, but there are still hundreds of thousands of reported infections each week [1]. Despite noted successes, drug therapies and available vaccines have only served to mitigate COVID-19. This, coupled with the uncertain evolution of the virus, necessitates a continued search for new and improved therapeutics and

*Correspondence:

Margaret A. Scull
scull@umd.edu
Jeffrey J. DeStefano
jdestefa@umd.edu

¹ Department of Cell Biology and Molecular Genetics, Maryland Pathogen Research Institute (MPRI), University of Maryland, College Park, MD 20742, USA

² Division of Immunology, Virginia-Maryland College of Veterinary Medicine, University of Maryland, College Park, MD 20742, USA



© The Author(s) 2023. **Open Access** This article is licensed under a Creative Commons Attribution 4.0 International License, which permits use, sharing, adaptation, distribution and reproduction in any medium or format, as long as you give appropriate credit to the original author(s) and the source, provide a link to the Creative Commons licence, and indicate if changes were made. The images or other third party material in this article are included in the article's Creative Commons licence, unless indicated otherwise in a credit line to the material. If material is not included in the article's Creative Commons licence and your intended use is not permitted by statutory regulation or exceeds the permitted use, you will need to obtain permission directly from the copyright holder. To view a copy of this licence, visit <http://creativecommons.org/licenses/by/4.0/>. The Creative Commons Public Domain Dedication waiver (<http://creativecommons.org/publicdomain/zero/1.0/>) applies to the data made available in this article, unless otherwise stated in a credit line to the data.

vaccines that may be applied to SARS-CoV-2 or other coronaviruses that may arise in the future.

A novel approach being pursued by several groups is the development of aptamers that can be employed as therapeutics or in diagnostics. Aptamers are short nucleic acid-based sequences that bind targets with high affinity and are typically produced using systematic evolution of ligands by exponential enrichment (SELEX) [2, 3]. Aptamers have the potential to block virus entry into cells or detect specific viruses in diagnostic assays (reviewed in [4, 5]). Several groups have produced DNA aptamers that bind to the SARS-CoV-2 S1 protein (a subunit of the viral spike protein found on the outer surface of the virus envelope) and block the interaction between the receptor binding domain (RBD) of S1 and the host cell receptor, angiotensin-converting enzyme 2 (ACE2) [6–16]; (Reviewed in: [17, 18]). Blocking this interaction prevents virus entry into cells, similar to how current neutralizing antibody therapies block SARS-CoV-2 infection (Reviewed in [19]). We previously reported the analysis of aptamer FANA-R8-9, which was made from 2'-fluoro-arabino nucleic acid (FANA) and was able to block the interaction between the viral RBD and ACE2 [15]. FANA is a xeno-nucleic acid (XNA), where XNAs are synthetic nucleic acids with altered sugar, base, or phosphate backbones. These alternatives to DNA and RNA aptamers often have advantageous properties as they may accommodate unique structures, have low immunogenicity, and have greater resistance to degradation [19–24].

Still, whether FANA-R8-9 can block spike-ACE2 interaction in the context of a viral particle, and whether FANA-R8-9—or any spike-targeting aptamer, to our knowledge—can function to block SARS-CoV-2 infection in the native respiratory microenvironment remains unknown. Notably, human airway epithelial (HAE) cultures at air-liquid interface have been established and recapitulate both the morphology and physiology of the airway epithelium in vivo, including the establishment of a mucus barrier [25, 26]. Importantly, these cultures are susceptible to SARS-CoV-2 and have been previously used to assess the efficacy of other antivirals against SARS-CoV-2 replication in vitro [27, 28]. Here, we report that FANA-R8-9 not only inhibits the uptake of spike-bearing pseudovirus particles, but also blocks SARS-CoV-2 infection in the HAE system, demonstrating the potential utility of XNA aptamers to target respiratory viruses in the mucosal microenvironment.

Materials and methods

Generation of aptamers

FANA-R8-9 was previously selected for binding to the SARS-CoV-2 spike RBD (Arg319-Phe541; Wuhan strain)

through SELEX [15]. FANA-R8-9 and various controls were produced by enzymatic synthesis using DNA templates and D4K polymerase [21], as previously described [15]. The DNA templates were 18 nucleotides longer than the products, allowing separation on denaturing acrylamide gels. Sequences are shown below with underlined bases composed of FANA and non-underlined DNA. FANA-R8-9: 5'-AAAAGGTAGTGCTGAATTCGCGA GCCCCGAUGAAAAGGGGAGAUAAAAUAUCUG UCGAUUCGCUAUCCAGUUGGCCU-3'; Scrambled FANA: 5'-AAAAGGTAGTGCTGAATTCG(N)40UUC GCUAUCCAGUUGGCCU-3' (N-FANA A, U, C or G); Fixed FANA (an unrelated sequence derived from the starting pool for SELEX): 5'-AAAAGGTAGTGCTGAATTCGAGUCACGCCAACACAGGAAGCGUAGGU CUAUCUUGUAGGUUCGCUAUCCAGUUGGCCU-3'; Fixed DNA (A DNA only copy of Fixed FANA): 5'-AAAAGGTAGTGCTGAATTCGAGTCACGCCAACACAGGAAGCGTAGGTCTATCTTGTAGGTTTC GCTATCCAGTTGGCCT-3'; IN-1.1 (FANA Human Immunodeficiency Virus (HIV)-1 integrase aptamer [29]: 5'-AAAAGGTAGTGCTGAATTCGUUCAA GUGUAUAUUAACUACGCAUCUUUCCCCUGCGU AUUCGCUAUCCAGUUGGCCU-3'. After extracting sequences from gels and recovery, the material was run over a Sephadex G-25 column to remove impurities. All sequences were quantified using absorbance at 260 nM assuming that FANA nucleotides absorb like DNA.

Cell lines and human airway epithelial cultures

Vero-E6 (with high expression of endogenous ACE2, Cat No. NR-53,726) were obtained from the Biodefense and Emerging Infections Research Resources Repository (BEI Resources, Manassas, VA, USA). Vero-E6 cells were maintained in complete Dulbecco's Minimal Essential Medium (DMEM; Invitrogen Life Technologies), supplemented with 10% fetal bovine serum (FBS) only, or 10% FBS plus 2 mM L-glutamine, nonessential amino acids, 100 units/ml of penicillin, 100 µg/ml of streptomycin, and 250 ng/ml of amphotericin B. Vero-E6 cells routinely tested negative for Mycoplasma sp. by real-time PCR.

Human airway tracheobronchial epithelial cells isolated from airway specimens from donors without underlying lung disease were provided by Lonza, Inc. Primary airway cells derived from single patient sources were first expanded on plastic in Pneumacult-Ex Plus medium (Cat No. 05040, StemCell Technologies), then seeded (3.3×10^4 cells/well) on rat tail collagen type 1-coated permeable Transwell® membrane supports (6.5 mm; Cat No. 3470, Corning, Inc.). Cultures were differentiated in Pneumacult-ALI medium (Cat No. 05001, StemCell Technologies) with the provision of an air-liquid interface for approximately 6 weeks to form polarized cultures

that resemble in-vivo pseudostratified mucociliary epithelium. All cell cultures were maintained at 37 °C with 5% CO₂. All experiments involving HAE cultures utilized at least two different donors, and the data in the figures are indicative of unique biological replicates.

Generation of spike-bearing pseudovirus particles and SARS-CoV-2 virus

The spike-bearing pseudovirus particles (rVSVΔG/SARS-CoV-2-S-D614Gd21-NLucP; Cat No. EGA298-PM, Kerastat, Inc.) were previously described [30] and obtained commercially for this study. In this recombinant vesicular stomatitis virus (VSV), the native glycoprotein gene has been replaced with the SARS-CoV-2 spike gene from the Wuhan strain lacking the last 21 residues of the cytoplasmic tail and containing an amino acid change (D614G) to promote the incorporation of the spike protein. This virus was propagated once in Vero-E6 cells and quantified by endpoint dilution (Tissue Culture Infectious Dose (TCID₅₀)) assay in Vero-E6 cells.

SARS-CoV-2 ancestral strain hCoV-19/USA/NY-PV08410/2020 (referred to as wild type and abbreviated as WT, Cat No. NR-53514) and Delta strain hCoV-19/USA/PHC658/2021(B.1.167.2) (Cat No. NR-55611) were obtained from BEI Resources with the permission of the Centers for Disease Control and Prevention (CDC). Viruses from BEI Resources were passaged in Vero-E6 cells cultured in a medium with reduced (1%) FBS. At 72 h post-infection, tissue culture supernatants were collected and clarified before being aliquoted and stored at -80 °C. The virus stocks were titrated using the TCID₅₀ assay. All experiments using live SARS-CoV-2 were performed in an approved Animal Biosafety Level 3+ (ABSL3+) facility at the University of Maryland using appropriate powered air-purifying respirators (PAPR) and protective equipment.

Pseudovirus particle inhibition assays

Vero-E6 cells were seeded in a 96-well plate at a density of 1.4×10^4 cells/well and incubated overnight at 37 °C. The following day, an inoculum containing pseudovirus particles (stock titer = 3×10^6 TCID₅₀/ml, diluted 1:64 in final inoculum) and FANA-R8-9 or control aptamer (50 nM, with 2-fold dilutions to 0.78 nM final concentration) was prepared and incubated for 30 min at room temperature. The cell culture medium was then removed, and the inoculum (25 μl) was applied directly to the cells, followed by a 2-h incubation at 37 °C. Serum-free DMEM containing FANA-R8-9 or control aptamer at the matching concentration was then added to reach a final 100 μl volume in each well. Twenty-four hours later, luciferase activity in each well was quantified using the Nano-Glo® Luciferase Assay System (Cat No. N1120; Promega)

according to the manufacturer's protocol and a Berthold Centro XS³ LB 960 plate reader. Relative luciferase units (RLU) were then normalized to "no aptamer" to determine the percent inhibition.

Pseudovirus aptamer binding assay

Pseudovirus particles (stock titer 3×10^6 TCID₅₀/ml) were concentrated by ultracentrifugation through a 20% sucrose cushion. Briefly, approximately 2 ml of virus in DMEM supplemented with 10% FBS was mixed with 1.5 ml of phosphate buffered saline (PBS, 1.7 mM KH₂PO₄, 5 mM Na₂HPO₄, 150 mM NaCl, pH 7.4) and loaded into a centrifuge tube (Beckman Cat. No. 344057, 5 ml capacity). One milliliter of 20% sucrose in 20 mM HEPES pH 7.4, 150 mM NaCl was then underlaid into the centrifuge tube, and PBS was added to the top to ensure proper fill. Centrifugation was done for 2 hrs at 35,000 rpm using a Beckman SW 55 Ti rotor. The supernatant was carefully removed and the pellet, along with a small amount of remaining sucrose solution, was resuspended in 200 μl of PBS. Aliquots were stored at -80 °C. The binding assay was performed by mixing concentrated pseudovirus (0, 0.63, 1.25, 2.5, or 5 μl) with radiolabeled aptamer or controls (20 nM final concentration) in a total volume of 15 μl PBS. Reactions also contained 15 pmoles of unlabeled DNA competitor (5'-AAAAGGTAGTGCTGAATT CG(N)₄₀TTCGCTATCCAGTTGGCCT-3' (N- DNA A, T, C, or dGTP)). Samples were incubated at room temperature for 20 min, then 50 μg of heparin sulfate (in PBS) was added, and incubations were continued for 40 min. Competitor DNA and the heparin post-binding step were necessary to reduce background binding such that only tightly bound nucleic acids would remain associated with virus material. Samples were filtered through pre-wetted (25 mM Tris-HCL pH 7.5, 10 mM KCl) nitrocellulose filters (Whatman™ Protran™, 25 mm diameter, 0.45 μm pore size) and washed with 5 ml of the pre-wetting buffer at a rate of ~0.5 ml/s. Filters were quantified in a scintillation counter.

SARS-CoV-2 inhibition assays in HAE

HAE cultures were washed with PBS twice, for 15 min at 37 °C each time, on the apical surface, and provided with fresh Pneumacult-ALI medium immediately prior to inoculation. In experiments where virus was mixed with aptamer before inoculation, aptamers were reconstituted in water at 3 pmol/μl. Aptamer (1 μl; or water (vehicle control)) was then mixed with SARS-CoV-2 (29 μl; wild type stock titer was 8.51×10^6 TCID₅₀/ml; Delta stock titer was 5×10^6 TCID₅₀/ml) and incubated for 30 min at room temperature. After this, 20 μl of the inoculum mixture was added to the apical surface of appropriate cultures before returning them to the 37 °C incubator. The

viral inoculum was left on the culture for the duration of the experiment. At 24 and 48 h post-infection (hpi), 0.5 μ l of aptamer (or water) was mixed with 14.5 μ l PBS and 10 μ l added to the apical surface of corresponding cultures. All cultures (including an uninfected (mock) culture run in parallel) were fixed at 72 h post-inoculation in paraformaldehyde for 60 min prior to removal from the ABSL3, in alignment with IBC-approved protocols. An additional set of experiments was performed in which aptamer was added after virus inoculation (at 0, 2, or 6 hpi) and again at 24 and 48 h post-infection prior to fixing at 72 h, as above.

En face immunofluorescence staining

Fixed HAE cultures were washed twice in PBS prior to permeabilization with 2.5% triton X-100/PBS for 15 min. HAE cultures were then blocked with 3% bovine serum albumin (BSA)/PBS for 1 h. Primary antibody, specific for the SARS-CoV-2 nucleoprotein (clone 1C7, Cat No. bsm-41411 M, Bioss), was then applied to the apical surface at a 1:500 dilution in 1% BSA/PBS and incubated overnight at 4 °C. Following three washes with PBS, a secondary antibody (donkey anti-mouse IgG Alexa Fluor 488, Cat No. A21202, Invitrogen) was diluted 1:500 in 1% BSA/PBS and applied to the apical surface for 1 h at room temperature. Cultures were then washed three times with PBS and viral antigen was visualized, and images were acquired with either a Zeiss Axio Observer 3 inverted fluorescence microscope or a Zeiss Axio Observer Z1 microscope with motorized stage, both equipped with Zeiss AxioCam 503 mono cameras and Zen imaging software, including the Tiles and Positions module. A Fiji macro was used to analyze whole culture composite images, or 4–5 images from pre-determined regions of the culture per replicate well to determine the percent antigen-positive area. The data were exported to Excel, and the average percent antigen-positive area was calculated per replicate. The resulting area quantification was then visualized in GraphPad Prism.

Aptamer degradation assays

Apical secretions from HAE cultures were harvested by adding 100 μ l of PBS to the culture surface and incubating at 37°C for 15 min before collection in a microcentrifuge tube with a pipette. Washes were stored at 4°C before use or used immediately for aptamer degradation testing. Apical washes from several donors were used in independent experiments and yielded similar results. Assays were conducted by adding 5' -³²P-labeled FANA-R8-9 or DNA-R8-9 (100 nM final concentration) directly to apical wash material in a total volume of 100 μ l. A 10 μ l aliquot was removed for digestion with DNaseI (2 U) for 2 h at 37 °C. After digestion, 10 μ l of 2 \times proteinase K digestion buffer

(100 mM Tris-HCl pH 7.5, 100 mM NaCl, 20 mM EDTA pH 8, 10 mM DTT, 2% (w:v) SDS) was added to the sample, which was then frozen at –80 °C. A second 10 μ l was removed as a “time 0” control and mixed with the same buffer. The remaining 80 μ l was incubated at 37 °C and 10 μ l aliquots were removed and placed in buffer at 0.5, 1, 2, 4, 8, or 24 h. The sample tube was briefly centrifuged before aliquot removal to bring all liquid to the bottom. Frozen samples were thawed and 20 μ g of proteinase K was added and samples were incubated in a PCR machine at 50 °C for 8 h. Twenty μ l of 2 \times gel loading buffer (90% formamide, 10 mM EDTA pH 8, 0.025% each bromophenol blue and xylene cyanol) was added to each sample and samples were electrophoresed on a 10% polyacrylamide-7 M urea gel in Tris-Borate-EDTA buffer as described [31]. Gels were dried and then imaged using an Amersham Typhoon phosphorimager.

Evaluation of cytotoxicity

To assess the direct effect of FANA-R8-9 on HAE culture integrity, cultures were washed twice with PBS and aptamer applied at 0, 24, and 48 h, as above (see “SARS-CoV-2 inhibition assays in HAE”). At 72 h post-initial aptamer application, 100 μ l of PBS was added to the apical surface, incubated for 30 min at 37 °C, and then collected and used to quantify lactate dehydrogenase (LDH) release (in a 50 μ l aliquot) using the CytoTox 96 Non-Radioactive Cytotoxicity Assay kit (Cat No. G1780, Promega) according to the manufacturer’s protocol. The basolateral media was then replaced with 500 μ l PBS and another 200 μ l PBS applied to the apical surface before measuring the transepithelial electrical resistance (TEER) using the Millicell Electrical Resistance System (ERS)-2 (Sigma). Following TEER measurements, PBS was removed and HAE cultures were fixed in 4% paraformaldehyde prior to paraffin embedding and sectioning at the New York University Experimental Pathology Research Laboratory (New York, NY, USA). Five micrometer-thick sections on slides were stained with hematoxylin and eosin (H&E) to allow histological evaluation of the epithelium by light microscopy. Images of H&E-stained sections were acquired using a Zeiss Axio Observer Z1 microscope and AxioCam Erc5s camera.

Statistical analysis

Statistical analysis of resulting data was done using Prism GraphPad v.9 software (GraphPad) and is further detailed in the figure legends.

Results

FANA Aptamer R8-9 inhibits SARS-CoV-2 pseudovirus particle uptake in cell lines

We previously demonstrated that FANA aptamer R8-9 could block the binding of ACE2 to the spike protein

receptor binding domain [15]. Thus, to further explore the ability of FANA-R8-9 to inhibit SARS-CoV-2 infection, we sought to determine whether FANA-R8-9 could block spike protein-mediated uptake of pseudoviral particles into cells. To do so, we utilized luciferase-expressing, VSV-based pseudovirus particles bearing the spike protein from the Wuhan strain. Pseudovirus particles were mixed with FANA-R8-9, or other aptamer controls, prior to inoculation of Vero-E6 cells, and luciferase expression was measured at 24 h post-inoculation as a proxy of successful pseudovirus particle entry. Pseudovirus signal decreased with increasing concentrations of FANA-R8-9, with a near complete block of infection at 50 nM (Fig. 1A). Various control aptamers also inhibited the pseudovirus signal, with the FANA-IN-1.1 and Fixed FANA aptamers demonstrating higher levels of inhibition than the Fixed DNA aptamer. Since this assay measures the expression of pseudovirus genomic products, both entry and virus replication are required for a signal. Thus,

FANA could possibly affect either or both of these steps in the viral life cycle, leading to the inhibition observed with FANA-IN-1.1 and Fixed FANA controls. A direct block of entry is most easily explained by the binding of the aptamer to the pseudovirus spike protein. To test the binding of FANA-R8-9 and control aptamers to the pseudovirus particles, the assay depicted in Fig. 1B was used. Concentrated pseudovirus particles were mixed and incubated with radiolabeled aptamer along with excess nonspecific DNA (unlabeled) of the same size. Heparin was then added and incubation continued for 40 min before processing the material for binding to nitrocellulose filters, which would retain the labeled aptamer only if bound to protein. The inclusion of nonspecific DNA and incubation with heparin, a binding competitor for nucleic acid, was required to decrease background binding to material in the pseudovirus preparation. Under these conditions, only nucleic acids that bind with high stability to the protein material in the pseudovirus preparation

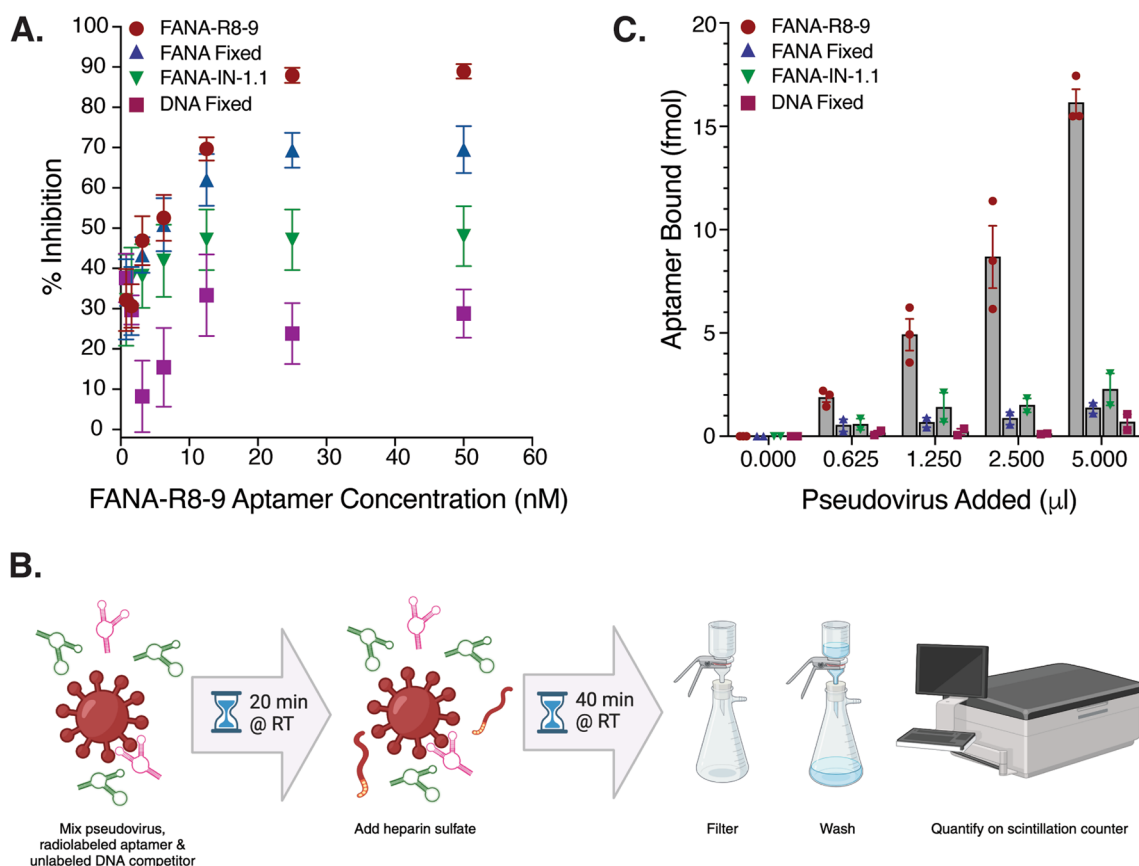


Fig. 1 Interaction between FANA-R8-9 and SARS-CoV-2 spike-bearing pseudovirus particles. **A** Aptamer-mediated inhibition of pseudovirus particle uptake in Vero E6 cells. Data shown represent the mean of 6–12 replicates per condition, combined across three (Fixed DNA; FANA-IN-1.1), four (Fixed FANA), or six (FANA-R8-9) experiments ± SEM. **B** Cartoon schematic of the experimental workflow utilized to generate the data in panel C. Radiolabeled FANA-R8-9 (pink); unlabeled DNA competitor (green). RT = room temperature. Created with BioRender.com. **C** Quantification of FANA-R8-9 (or control) aptamer bound to increasing amounts of SARS-CoV-2 spike-bearing pseudovirus particles. Data shown represent the mean of single replicates per condition, combined across two (Fixed FANA; FANA-IN-1.1; Fixed DNA) or three (FANA-R8-9) experiments ± SEM

would be measurable. Results showed that FANA-R8-9 bound in a concentration-dependent manner to pseudovirus material while the controls showed weak binding (Fig. 1C). These data suggest that only FANA-R8-9 interacts strongly with spike protein in the context of a viral particle. The inhibition observed with FANA controls is likely the result of a mechanism that does not involve binding to the pseudovirus spike protein.

FANA-R8-9 inhibits SARS-CoV-2 infection in HAE cultures

Given the ability of FANA-R8-9 to bind pseudovirus particles harboring the SARS-CoV-2 spike protein and inhibit their entry, we next asked if this aptamer could block SARS-CoV-2 virus infection in a model of human airway epithelium that recapitulates infection in a more physiologically-relevant setting. Normal human tracheobronchial cells from individual donors were differentiated on Transwell® membrane supports at air-liquid interface and mucus secretions were removed prior to inoculation to facilitate infection. Preliminary tests indicated that FANA-R8-9 concentrations less than 100 nM were associated with stochastic SARS-CoV-2 inhibition in HAE (data not shown); thus, 100 nM aptamer was utilized in all subsequent assays. In initial experiments, 100 nM FANA-R8-9, or water as a vehicle control, was mixed with virus prior to inoculation of the apical culture surface (with an approximate multiplicity of infection of 1). Additional aptamer was added to corresponding cultures at 24 and 48 hpi, and the extent of infection across the epithelium was evaluated at 72 hpi following en face staining for viral antigen and fluorescence microscopy (Fig. 2A). To further assess the ability of the aptamer to inhibit more recent variants, we performed these experiments with both the wild-type strain (hCoV-19/USA/NY-PV08410/2020) and Delta variant (hCoV-19/USA/PHC658/2021(B.1.167.2)). Notably, FANA-R8-9 significantly reduced the nucleocapsid-positive area in HAE following infection with either strain, indicating fewer cells were infected in the presence of the aptamer (Fig. 2B, D).

We next sought to assess the ability of FANA-R8-9 to act in a “therapeutic” setting, by adding the aptamer directly to the apical surface of HAE cultures after virus inoculation. We selected the Delta variant for these assays since FANA-R8-9 was able to completely block infection with this virus in our initial experiments (Fig. 2B). Delta was added to the apical surface of HAE and FANA-R8-9 was applied either immediately (0), or 2, or 6 hpi, followed by additional aptamer treatments at 24 and 48 hpi. While infection could be detected at 72 hpi in some FANA-R8-9-treated cultures, the viral nucleoprotein-positive area in FANA-R8-9-treated HAE was still significantly reduced compared to HAE without aptamer

treatment (Fig. 2C). These data indicate that FANA-R8-9 can interact with SARS-CoV-2 and limit infection within the airway mucosal environment even several hours after viral infection. The treatment window was not indefinite, however, since adding FANA-R8-9 to Delta-inoculated HAE cultures 24 hpi did not significantly impact the infection (data not shown).

Inhibition of SARS-CoV-2 Infection in HAE is specific to FANA-R8-9

In our pseudovirus particle inhibition assays (Fig. 1A), we noted that other aptamers could limit pseudovirus particle uptake and/or luciferase expression in Vero-E6 cells, though not to the same extent as FANA-R8-9. To verify the specificity of Delta variant inhibition by FANA-R8-9 in HAE, we assayed FANA Fixed, FANA scramble, and DNA Fixed aptamers in parallel with FANA-R8-9 in the Fig. 2A workflow. Consistent with our previous results (Fig. 2B, C), FANA-R8-9 completely blocked Delta variant infection (Fig. 3) when the viral antigen-positive area was assessed at 72 hpi. In contrast, none of the other control aptamers significantly affected SARS-CoV-2 infection indicating that FANA-R8-9-mediated inhibition is specific to the FANA-R8-9 sequence.

FANA-R8-9 is stable in apical secretions from HAE cultures and does not induce overt toxicity

We previously demonstrated that FANA-R8-9 remained intact for several hrs in serum-containing cell culture media, and had a breakdown rate approximately equal to a similar DNA aptamer [15]. To assess FANA-R8-9 stability in airway mucus, we harvested apical secretions from HAE cultures and monitored FANA-R8-9 decay over 24 h in these secretions, or in DMEM culture media supplemented with 10% FBS for comparison (Fig. 4). The latter condition mimics the previous results noted above and demonstrates modest, though clear decay over 24 h. In contrast, FANA-R8-9 was more stable in HAE secretions, showing a very slight breakdown only after 24 h. The results indicate that FANA-R8-9 retains potency in HAE cultures from several hrs to days.

Given the lack of FANA-R8-9 degradation in HAE secretions, we next sought to determine if FANA-R8-9 demonstrated any overt toxicity in HAE cultures using two types of cell toxicity assays, conducted with 100 and 1000 nM aptamer. The latter concentration is 10× greater than the maximum concentration in virus inhibition assays. HAE cultures were first treated with aptamer using the same timing and conditions employed in infection assays. This was followed by toxicity assays that use lactate dehydrogenase (LDH) release as a proxy for cell death and transepithelial

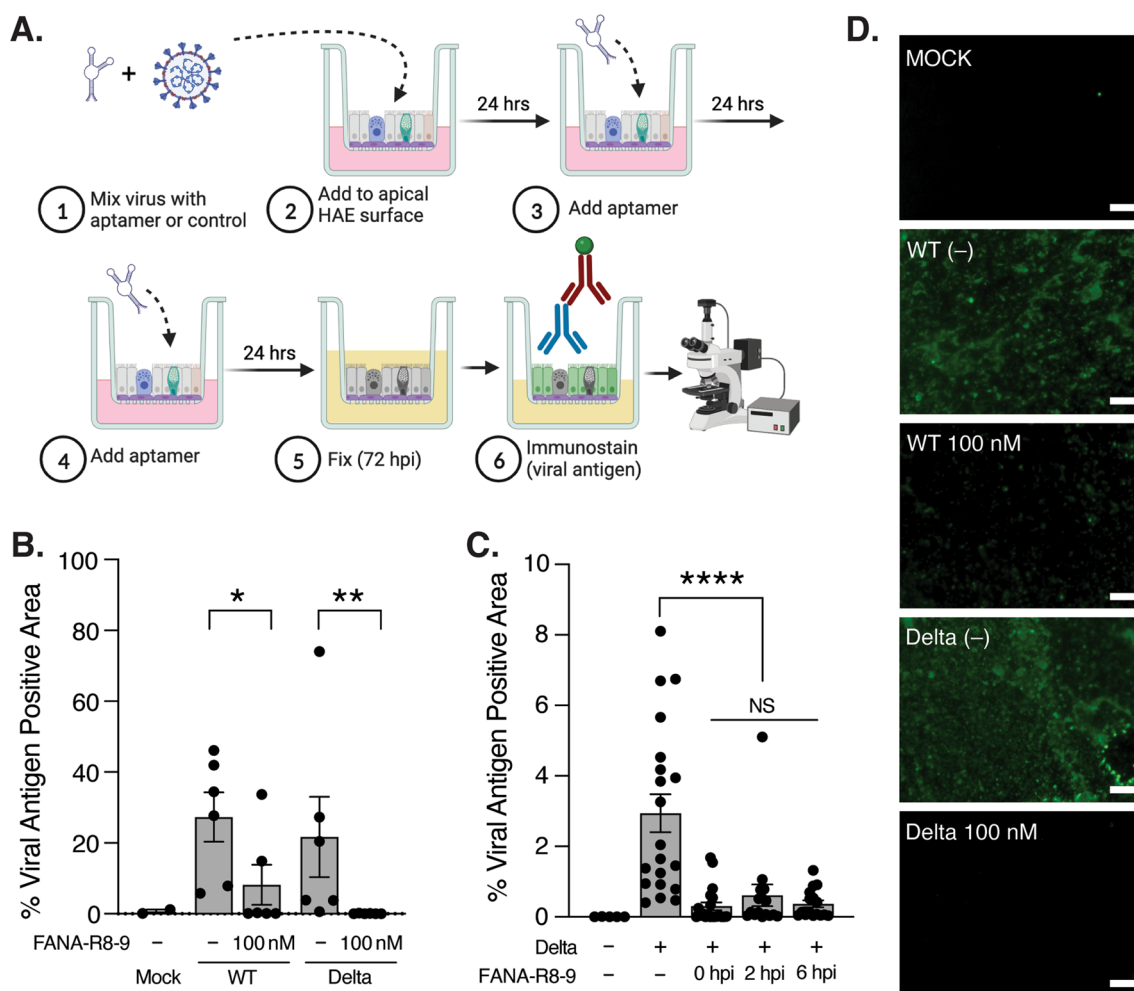


Fig. 2 FANA-R8-9 aptamer inhibits SARS-CoV-2 infection in HAE cultures. **A** Cartoon schematic of the experimental workflow used to obtain the data in panel B. Created with BioRender.com. Hours post-infection = hpi. **B** The percent viral antigen positive area, quantified following en face immunofluorescence staining and imaging in HAE cultures infected with WT SARS-CoV-2 or Delta variant in the presence or absence of FANA-R8-9 aptamer. Individual biological replicates across two experiments (n = 3 per donor; 2 donors) are shown with the bar representing the mean ± SEM. Experimental results were analyzed by the Mann–Whitney test between indicated conditions. All data are significant where indicated (*p < 0.05; **p < 0.005). **C** The percent viral antigen positive area determined as in panel B for cultures that were first inoculated with the Delta variant, then subsequently treated with vehicle or FANA-R8-9 aptamer immediately following virus inoculation (0), or 2, or 6 hpi. FANA-R8-9 aptamer was added to the indicated cultures again at 24 and 48 hpi prior to fixation at 72 hpi and analysis by en face immunostaining and fluorescence microscopy as in **A** and **B**. Individual biological replicates for one experiment (n = 4 per donor; 4–5 donors per condition) are shown with the bar representing the mean ± SEM. Experimental results were analyzed using ordinary one-way analysis of variance (ANOVA) between indicated conditions. Data are non-significant (NS) or significant where indicated (****p < 0.0001). **D** Representative photomicrographs of HAE cultures analyzed in panel B. HAE were fixed at 72 hpi and immunoprobed en face for the presence of SARS-CoV-2 nucleoprotein (green) after apical inoculation with vehicle (mock) or SARS-CoV-2 (WT or Delta variant) in the presence (100 nM) or absence (-) of FANA-R8-9 aptamer. Scale bar = 100 μm.

electrical resistance (TEER) as a measure of epithelial barrier integrity. Notably, both LDH release (Fig. 5A) and TEER (Fig. 5B) assays demonstrated no significant toxicity at 100 or 1000 nM aptamer. These results were further supported by a lack of overt cytopathology in histological cross-sections of HAE and are consistent with the low toxicity observed with FANA oligonucleotides in cell culture by others (Fig. 5C) [32, 33].

Discussion

Since the emergence of SARS-CoV-2, a variety of therapeutics have been utilized to inhibit viral replication and mitigate disease severity including immune modulators, monoclonal antibodies, and antiviral drugs such as remdesivir, molnupiravir, and nirmatrelvir with ritonavir. Nonetheless, developing novel strategies to block SARS-CoV-2, as well as other viral infections for which targeted antivirals do not exist, is paramount. Here, we have

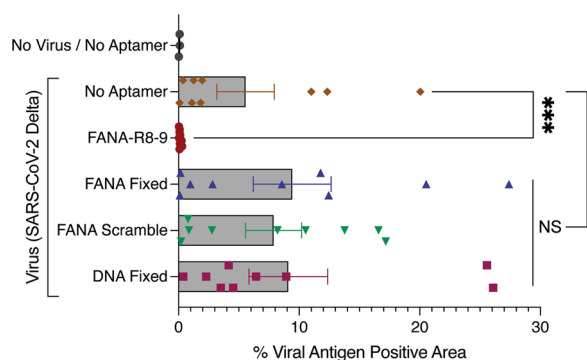


Fig. 3 FANA-R8-9 aptamer-mediated inhibition of SARS-CoV-2 infection in HAE cultures is sequence-specific. HAE cultures were inoculated with the indicated treatments at 0, 24, and 48 h, (as outlined in Fig. 2A), then fixed at 72 h. The percentage of viral antigen-positive area was then quantified following *en face* immunofluorescence staining and imaging of SARS-CoV-2 nucleoprotein in fixed cultures. Individual biological replicates are shown ($n=3$ replicates per condition, per donor; 2 donors (1 donor was assayed twice, in independent experiments) with the bar representing the mean \pm SEM. Experimental results were analyzed using the Mann-Whitney test (between No Aptamer and FANA-R8-9 conditions) or one-way ANOVA (between No Aptamer and all aptamer controls) and data are non-significant (NS) or significant (***) $p < 0.001$ where indicated

focused on aptamer technology, which has proven useful in diagnostics [34–36] and demonstrated clinical success with the approval of pegaptinib (Macugen) for treating age-related macular degeneration in 2004. Aptamers specific for viral targets (e.g., polymerases, integrases, helicases) have also been selected, with some demonstrating antiviral activity (Reviewed in [4, 5]). However, aptamers do not efficiently enter cells. Therefore, while aptamer uptake into cells can be improved through interaction with cell surface proteins [37–39] or by coupling to cell-penetrating peptides [40, 41], aptamers that target viral surface proteins are likely more feasible as antivirals.

Recently, several aptamers to the spike protein of SARS-CoV-2 have been characterized ([6–16]; Reviewed in: [17, 18]). The majority are composed of DNA with the exceptions being a coupled peptide/DNA aptamer [42], an RNA/2'-fluoro RNA (F-RNA) mixed aptamer [9], and the FANA R8-9 aptamer used in this research [15]. The XNA composition of the latter two aptamers could confer some advantages over natural nucleic acid aptamers (see "Background"), although this remains to be determined. Notably, our pseudovirus infections in Vero cells indicated that FANA controls (Fixed FANA and FANA-IN-1.1) were more inhibitory than DNA (Fixed DNA), but less inhibitory than FANA-R8-9. However, none of these controls exhibited stable binding to pseudovirus material, or a significant effect on SARS-CoV-2 infection in our HAE assays.

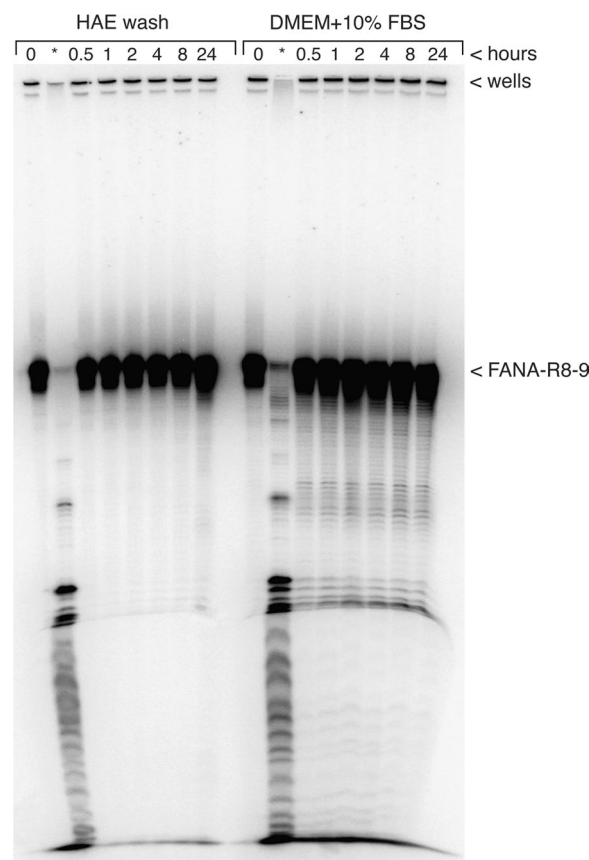


Fig. 4 FANA-R8-9 aptamer is stable in apical secretions from HAE cultures. Degradation of FANA-R8-9 aptamer in HAE and serum-supplemented DMEM. Radiolabeled FANA-R8-9 aptamer was incubated in HAE washes or serum-supplemented DMEM medium as described in Materials and Methods. Aliquots were removed at the indicated time points and processed as described, then run on a 10% denaturing polyacrylamide-urea gel. The dried gel was exposed and imaged with a phosphorimager. A small amount of material remained in the wells during electrophoresis. The position of the aptamer (~79 nts) is indicated. *An aliquot of the sample was digested with 2 U of DNase I for 2 h in the indicated medium

One explanation is that the “weak” binding of FANA to the pseudovirus, that cannot be measured in the assay, is enough to interfere with entry, thus leading to a lower signal. A second possibility is that FANA interferes with replication or transcription of the VSV-derived virus. Remarkably, while studying the ability of HIV genome-targeting FANA antisense oligonucleotides (ASOs) to block HIV infection, researchers not only observed sequence-specific inhibition of HIV infection, but also a non-specific inhibitory component [32]. Furthermore, the inhibitory nature of catabolic metabolites of FANA oligonucleotide, including 2'-deoxy-2'-fluoroarabinonucleosides, against some viruses has been reported [43–45]. Consistent with these previous

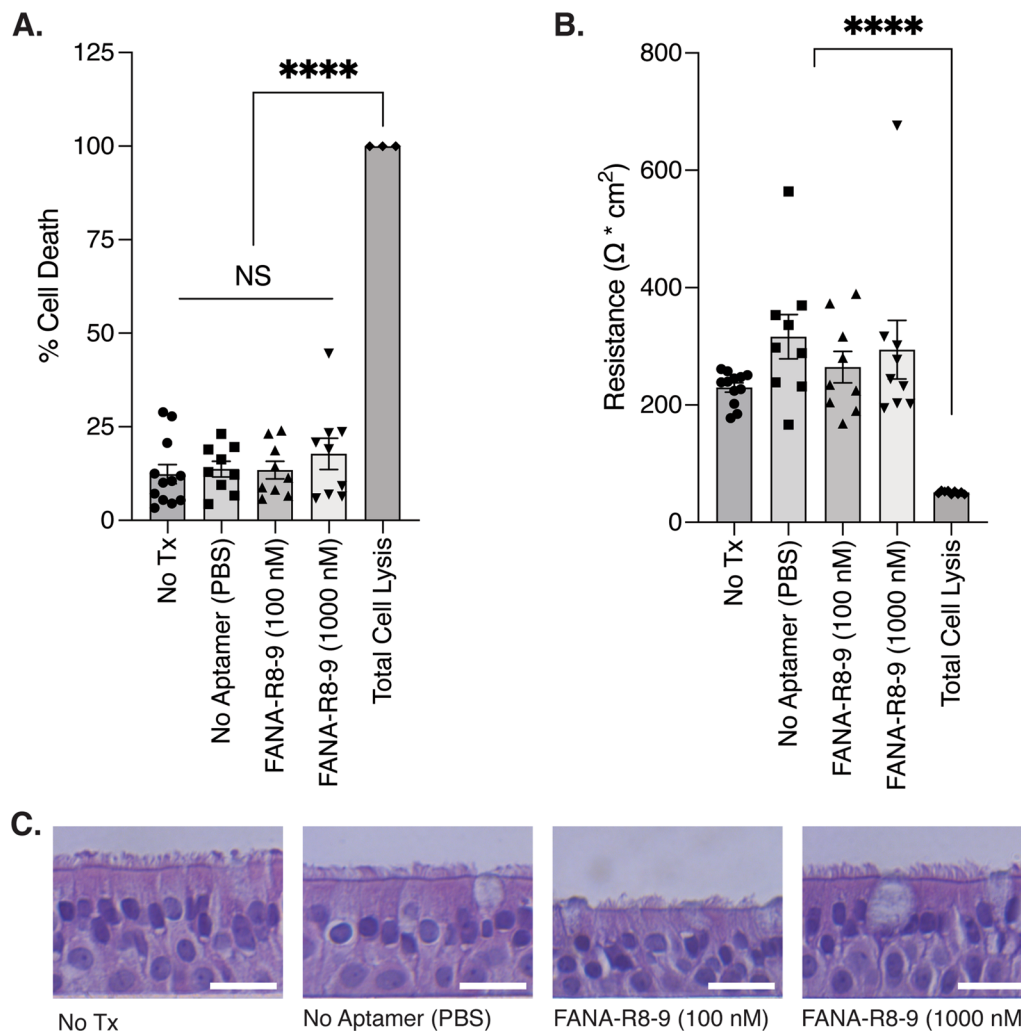


Fig. 5 A lack of overt cytopathic effects in HAE cultures following FANA-R8-9 aptamer treatment. To quantify aptamer-induced cytopathic effects, HAE cultures were first inoculated with the indicated treatments at 0, 24, and 48 h, (as outlined in Fig. 2A). Lactate dehydrogenase (LDH) released into the apical compartment was then quantified at 72 h and cell death was calculated as a percent of the average total cell lysis control (**A**). Transepithelial electrical resistance (TEER) was then determined in the same cultures (**B**) prior to fixation. Individual biological replicates from two experiments are shown in A and B ($n = 3-4$ replicates per condition, per donor; 3 donors) with the bar representing the mean \pm SEM. Experimental results were analyzed using one-way ANOVA and data are non-significant (NS) or significant ($****p < 0.0001$) where indicated. **C** Representative histological cross-sections of HAE cultures fixed after TEER measurement for one donor. H&E counterstain. Scale bar = 20 μm

reports, we have also observed sequence-independent inhibition of HIV by FANA nucleic acids similar in size to FANA-R8-9 and the controls used in the current experiments. Although the cause of the observed non-specific inhibition of pseudovirus infections in Vero cells remains unclear, the potential useful antiviral effects of FANA and other XNAs warrant further analysis.

Importantly, beyond potential XNA-mediated effects, SARS-CoV-2 spike aptamers have been shown to block pseudovirus or live virus [9] infections in cell culture and the respiratory tract of ACE2 transgenic mice [16].

However, there is a clear need to examine aptamers in models that more closely mimic human physiology, an approach already being used to test other potential SARS-CoV-2 inhibitors [46]. Here, we have extended our previous work and demonstrated FANA-R8-9 is not only capable of blocking spike-bearing pseudovirus particles, but also SARS-CoV-2 infection in a physiologically-relevant model of human airway epithelium. FANA-R8-9 was able to reduce infection when mixed with virus prior to inoculation and several hours after viral infection. To the extent that the HAE model mimics the human airway, this suggests that administering aptamer after infection

could prevent virus spread and highlights the potential for using aptamers to treat COVID-19 and other respiratory infections. Notably, we did not observe any cytopathic effects, gross morphological changes, or loss of epithelial barrier integrity after 72 h of aptamer treatment. While these data are not surprising since we do not expect FANA-R8-9 to be readily taken up by the epithelial cells in the HAE model, the impacts of FANA or FANA-R8-9 on the mucus barrier and underlying cells remain to be fully characterized.

SARS-CoV-2 spike, like other viral glycoproteins, is a primary target of the humoral immune response which can drive glycoprotein sequence evolution over time. As a result, aptamers selected against the glycoprotein (spike) of one virus strain may not inhibit others. Here, FANA-R8-9 was initially selected for binding to the Wuhan virus RBD; however, our data indicate that FANA-R8-9 also effectively inhibits the Delta variant. Indeed, FANA-R8-9 has significantly stronger binding affinity to Delta RBD (23.5 ± 4.6 nM vs. 1.4 ± 0.4 nM, for Wuhan and Delta, respectively) [14]. This enhanced binding may explain why FANA-R8-9 was even more potent against Delta in the HAE assays, although FANA-R8-9 significantly inhibited both strains. Notably, the RBD domains of Wuhan and Delta differ by only 2 amino acids (L452R and T478K) with the changes in Delta resulting in two additional positive charges in the RBD. These additional charges may help enhance the binding of nucleic acid which is strongly negatively charged. In contrast to Delta, Omicron variants typically have a dozen or more amino acid changes in the RBD compared to Wuhan and FANA-R8-9 binds much less strongly to Omicron RBD. We are currently working on producing FANA aptamers to Omicron RBD and S1 domains.

Conclusions

Overall, nucleic acids as therapeutics have been under rapid development with several FDA-approved drugs and more in the pipeline (reviewed in [47–49]). Most have been small interfering RNAs (siRNAs), ASOs, splice switching RNAs, or mRNAs. To date, siRNA and ASOs directed to respiratory targets have shown some efficacy in animal models. FANA-R8-9 toxicity and efficacy in animal models of SARS-CoV-2 infection remains unknown, but assessment of FANA-R8-9 *in vivo* is a logical next step. Still, these prior successes, in conjunction with our current data, promise further development of FANA-R8-9 and other virus-specific aptamers as therapeutics in the near future.

Acknowledgements

We thank Philipp Holliger (Cambridge Biomedical Campus, Cambridge, UK) for the D4K enzyme used to make FANA. We are also grateful to the directors, managers, and staff of the New York University Experimental Pathology

Research Laboratory. The following reagents were obtained through BEI Resources, NIAID, NIH: African Green Monkey Kidney Epithelial Cells (Vero E6) expressing high endogenous angiotensin-converting enzyme 2 (NR-53726); SARS-Related Coronavirus 2, isolate New York-PV08410/2020 (NR-53514); and SARS-Related Coronavirus 2, isolate hCoV-19/USA/PHC658/2021 (lineage B.1.617.2; Delta Variant; NR-55611), contributed by Drs. Richard Webby and Anami Patel.

Author contributions

NR generated aptamers, performed experiments (pseudovirus particle assays; en face staining and imaging of SARS-CoV-2 infection in HAE cultures; cytotoxicity assays in HAE cultures), analyzed and curated data. WL performed experiments with SARS-CoV-2 virus. MAI performed experiments (en face staining and imaging of SARS-CoV-2 infection in HAE cultures; imaging of H&E stained sections) and analyzed and curated data. JML prepared apical HAE culture secretions for use in degradation experiments. EIA prepared pseudovirus particles and established methods for pseudovirus particle assays. XZ supervised all ABSL3 work and acquired funding. MAS conceptualized the study, designed methods, supervised experiments utilizing HAE cultures, acquired funding, and wrote the manuscript. JJD conceptualized the study, designed methods, supervised the generation of aptamers and experiments utilizing pseudovirus particles, performed experiments (aptamer binding to pseudovirus particles; aptamer degradation assays), analyzed and curated data, acquired funding, and wrote the manuscript. All authors read and approved the final manuscript.

Funding

This research was funded by a University of Maryland Coronavirus Research Seed Grant to JJD and MAS and was also supported by the National Institute of Allergy and Infectious Diseases, Grant Number R21AI163816 to JJD, MAS, and XZ.

Availability of data and materials

All data generated or analyzed during this study are included in this published article.

Declarations

Ethics approval and consent to participate

Not applicable.

Competing interests

The authors declare no competing interests.

Received: 29 September 2023 Accepted: 30 October 2023

Published online: 07 November 2023

References

1. WHO Coronavirus (COVID-19) Dashboard. [cited 2023 Jul 12]. Available from: <https://covid19.who.int/>.
2. Ellington AD, Szostak JW (1990) In vitro selection of RNA molecules that bind specific ligands. *Nature* 346:818–22
3. Tuerk C, Gold L (1990) Systematic evolution of ligands by exponential enrichment: RNA ligands to bacteriophage T4 DNA polymerase. *Science* 249:505–10
4. Zou X, Wu J, Gu J, Shen L, Mao L. Application of aptamers in virus detection and antiviral therapy. *Front Microbiol.* 2019;10:1462.
5. Aptamers against viruses (2021) Selection strategies and bioanalytical applications. *Trends Analyt Chem* 143:116349
6. Song Y, Song J, Wei X, Huang M, Sun M, Zhu L et al (2020) Discovery of aptamers targeting the receptor-binding domain of the SARS-CoV-2 Spike Glycoprotein. *Anal Chem* 92:9895–900
7. Sun M, Liu S, Wei X, Wan S, Huang M, Song T, et al. Aptamer blocking strategy inhibits SARS-CoV-2 virus infection. *Angew Chem Int Ed Engl.* 2021;60:10266–72.

8. Sun M, Liu S, Song T, Chen F, Zhang J, Huang J-A et al (2021) Spherical neutralizing aptamer inhibits SARS-CoV-2 Infection and suppresses mutational Escape. *J Am Chem Soc* 143:21541–8
9. Valero J, Civit L, Dupont DM, Selnihhin D, Reinert LS, Idorn M, et al. A serum-stable RNA aptamer specific for SARS-CoV-2 neutralizes viral entry. *Proc Natl Acad Sci USA*. 2021;118:e2112942118. <https://doi.org/10.1073/pnas.2112942118>.
10. Liu X, Wang Y-L, Wu J, Qi J, Zeng Z, Wan Q et al (2021) Neutralizing aptamers Block S/RBD-ACE2 interactions and prevent host cell Infection. *Angew Chem Int Ed Engl* 60:10273–8
11. Kacheroovsky N, Yang LF, Dang HV, Cheng EL, Cardle II, Walls AC et al (2021) Discovery and characterization of Spike N-Terminal domain-binding aptamers for Rapid SARS-CoV-2 detection. *Angew Chem Int Ed Engl* 60:21211–5
12. Yang G, Li Z, Mohammed I, Zhao L, Wei W, Xiao H et al (2021) Identification of SARS-CoV-2-against aptamer with high neutralization activity by blocking the RBD domain of spike protein 1. *Signal Transduct Target Ther* 6:227
13. Li J, Zhang Z, Gu J, Stacey HD, Ang JC, Capretta A et al (2021) Diverse high-affinity DNA aptamers for wild-type and B.1.1.7 SARS-CoV-2 spike proteins from a pre-structured DNA library. *Nucleic Acids Res* 49:7267–79
14. Zhang Z, Li J, Gu J, Amini R, Stacey HD, Ang JC et al (2022) A universal DNA aptamer that recognizes spike proteins of Diverse SARS-CoV-2 variants of concern. *Chemistry* 28:e202200078
15. Alves Ferreira-Bravo I, DeStefano JJ. Xeno-Nucleic Acid (XNA) 2'-Fluoroarabino nucleic acid (FANA) aptamers to the receptor-binding domain of SARS-CoV-2 S protein block ACE2 binding. *Viruses*. 2021;13:1983.
16. Ayass MA, Tripathi T, Griko N, Pashkov V, Dai J, Zhang J et al (2022) Highly efficacious and safe neutralizing DNA aptamer of SARS-CoV-2 as an emerging therapy for COVID-19 Disease. *Virology* 19:227
17. Zhang Y, Juhas M, Kwok CK (2023) Aptamers targeting SARS-COV-2: a promising tool to fight against COVID-19. *Trends Biotechnol* 41:528–44
18. Chang ZY, Alhamami FAMS, Chin KL (2023) Aptamer-based strategies to address challenges in COVID-19 diagnosis and treatments. *Interdiscip Perspect Infect Dis* 2023:9224815
19. Jin D, Wei J, Sun J (2021) Analysis of the molecular mechanism of SARS-CoV-2 antibodies. *Biochem Biophys Res Commun* 566:45–52
20. Pinheiro VB, Holliger P (2012) The XNA world: progress towards replication and evolution of synthetic genetic polymers. *Curr Opin Chem Biol* 16:245–52
21. Pinheiro VB, Taylor AI, Cozens C, Abramov M, Renders M, Zhang S et al (2012) Synthetic genetic polymers capable of heredity and evolution. *Science* 336:341–4
22. Schmidt M, Pei L (2011) Synthetic toxicology: where engineering meets biology and toxicology. *Toxicol Sci* 120(Suppl 1):204–24
23. Zhang Y, Wang Z, Gemeinhart RA (2013) Progress in microRNA delivery. *J Control Release* 172:962–74
24. Watts JK, Katolik A, Viladoms J, Damha MJ (2009) Studies on the hydrolytic stability of 2'-fluoroarabinonucleic acid (2'-F-ANA). *Org Biomol Chem* 7:1904–10
25. Kesimer M, Kirkham S, Pickles RJ, Henderson AG, Alexis NE, Demaria G et al (2009) Tracheobronchial air-liquid interface cell culture: a model for innate mucosal defense of the upper airways? *Am J Physiol Lung Cell Mol Physiol* 296:L92–100
26. Gray TE, Guzman K, Davis CW, Abdullah LH, Nettesheim P (1996) Mucociliary differentiation of serially passaged normal human tracheobronchial epithelial cells. *Am J Respir Cell Mol Biol* 14:104–12
27. Sheahan TP, Sims AC, Zhou S, Graham RL, Pruijssers AJ, Agostini ML, et al. An orally bioavailable broad-spectrum antiviral inhibits SARS-CoV-2 in human airway epithelial cell cultures and multiple coronaviruses in mice. *Sci Transl Med*. 2020;12:eabb5883. <https://doi.org/10.1126/scitranslmed.abb5883>.
28. de Vries M, Mohamed AS, Prescott RA, Valero-Jimenez AM, Desvignes L, O'Connor R, et al. A comparative analysis of SARS-CoV-2 antivirals characterizes 3CL inhibitor PF-00835231 as a potential new treatment for COVID-19. *J Virol [Internet]*. 2021;95:e01819. <https://doi.org/10.1128/JVI.01819-20>.
29. Rose KM, Alves Ferreira-Bravo I, Li M, Craigie R, Ditzler MA, Holliger P et al (2019) Selection of 2'-Deoxy-2'-Fluoroarabino Nucleic Acid (FANA) Aptamers that bind HIV-1 integrase with Picomolar Affinity. *ACS Chem Biol* 14:2166–75
30. Havranek KE, Jimenez AR, Acciani MD, Lay Mendoza MF, Reyes Ballista JM, Diaz DA, et al. SARS-CoV-2 spike alterations enhance pseudoparticle titers and replication-competent VSV-SARS-CoV-2 virus. *Viruses*. 2020;12:1465. <https://doi.org/10.3390/v12121465>.
31. Sambrook J, Russell DW. *Molecular cloning: a laboratory manual*. 2001.
32. Takahashi M, Li H, Zhou J, Chomchan P, Aishwarya V, Damha MJ, et al. Dual mechanisms of action of self-delivering, anti-HIV-1 FANA oligonucleotides as a potential new approach to HIV therapy. *Mol Ther Nucleic Acids*. 2019;17:615–25.
33. Guimond A, Viau E, Aubé P, Renzi PM, Paquet L, Ferrari N (2008) Advantageous toxicity profile of inhaled antisense oligonucleotides following chronic dosing in non-human primates. *Pulm Pharmacol Ther* 21:845–54
34. Kumar Kulabhusan P, Hussain B, Yüce M. Current perspectives on aptamers as diagnostic tools and therapeutic agents. *Pharmaceutics*. 2020;12:646. <https://doi.org/10.3390/pharmaceutics12070646>
35. Ruiz Ciancio D, Vargas MR, Thiel WH, Bruno MA, Giangrande PH, Mestre MB. Aptamers as diagnostic tools in cancer. *Pharmaceutics*. 2018;11:86. <https://doi.org/10.3390/ph11030086>.
36. González VM, Martín ME, Fernández G, García-Sacristán A. Use of aptamers as diagnostics tools and antiviral agents for human viruses. *Pharmaceutics*. 2016;9:78. <https://doi.org/10.3390/ph9040078>.
37. McNamara JO 2, Andrechek ER, Wang Y, Viles KD, Rempel RE, Gilboa E et al (2006) Cell type-specific delivery of siRNAs with aptamer-siRNA chimeras. *Nat Biotechnol* 24:1005–15
38. Orava EW, Cicmil N, Gariépy J (2010) Delivering cargoes into cancer cells using DNA aptamers targeting internalized surface portals. *Biochim Biophys Acta* 1798:2190–200
39. Yoon S, Rossi JJ, Aptamers (2018) Uptake mechanisms and intracellular applications. *Adv Drug Deliv Rev* 134:22–35
40. McClure G, Banerjee S. Cell-penetrating peptides to enhance delivery of oligonucleotide-based therapeutics. *Biomedicines*. 2018;6:51. <https://doi.org/10.3390/biomedicines6020051>.
41. Anwar S, Mir F, Yokota T. Enhancing the effectiveness of oligonucleotide therapeutics using cell-penetrating peptide conjugation, chemical modification, and carrier-based delivery strategies. *Pharmaceutics*. 2023;15:1130. <https://doi.org/10.3390/pharmaceutics15041130>.
42. Lee M, Kang B, Lee J, Lee J, Jung ST, Son CY et al (2022) De novo selected hACE2 mimics that integrate hotspot peptides with aptameric scaffolds for binding tolerance of SARS-CoV-2 variants. *Sci Adv* 8:eabq6207
43. Watanabe KA, Reichman U, Hirota K, Lopez C, Fox JJ. Nucleosides. 110. Synthesis and antiherpes virus activity of some 2'-fluoro-2'-deoxyarabinofuranosylpyrimidine nucleosides. *J Med Chem*. 1979;22:21–4.
44. Kong XB, Scheck AC, Price RW, Vidal PM, Fanucchi MP, Watanabe KA, et al. Incorporation and metabolism of 2'-fluoro-5-substituted arabinosyl pyrimidines and their selective inhibition of viral DNA synthesis in herpes simplex virus type 1 (HSV-1)-infected and mock-infected vero cells. *Antiviral Res*. 1988;10:153–66.
45. Chu CK, Ma T, Shanmuganathan K, Wang C, Xiang Y, Pai SB, et al. Use of 2'-fluoro-5-methyl-beta-l-arabinofuranosyluracil as a novel antiviral agent for Hepatitis B virus and Epstein-Barr virus. *Antimicrob Agents Chemother*. 1995;39:979–81.
46. Do TND, Donckers K, Vangeel L, Chatterjee AK, Galloway PA, Bobardt MD et al (2021) A robust SARS-CoV-2 replication model in primary human epithelial cells at the air liquid interface to assess antiviral agents. *Antiviral Res* 192:105122
47. Egli M, Manoharan M (2023) Chemistry, structure and function of approved oligonucleotide therapeutics. *Nucleic Acids Res* 51:2529–73
48. Kulkarni JA, Witzigmann D, Thomson SB, Chen S, Leavitt BR, Cullis PR et al (2021) The current landscape of nucleic acid therapeutics. *Nat Nanotechnol* 16:630–43
49. Chen J, Tang Y, Liu Y, Dou Y (2018) Nucleic acid-based therapeutics for Pulmonary Diseases. *AAPS PharmSciTech* 19:3670–80

Publisher's Note

Springer Nature remains neutral with regard to jurisdictional claims in published maps and institutional affiliations.